JOURNAL OF MATERIALS SCIENCE 26 (1991) 2725–2730

Ambient gas-induced SiC-like structures in edge-defined film-fed grown polycrystalline silicon samples

B. PIVAC*, A. BORGHESI
Dipartimento di Fisica, Universita di Pavia, I-27100 Pavia, Italy
R. CANTERI, M. ANDERLE
IRST-Divisione di Scienza dei Materiali, I-38050 Povo, Trento, Italy

Several techniques were used to study a surface layer structure of edge-defined film-fed grown polycrystalline silicon samples grown in CO gas deliberately added to the purging atmosphere. Although infrared analysis reveals the presence of cubic SiC structures, other techniques, such as spectroscopic ellipsometry and Raman spectroscopy, do not detect its presence. It is concluded that a layer with specific structure, formed in the course of ribbon growth, consists of indiffused oxygen formed upon reaction of CO gas with molten Si. Indiffused oxygen, in turn, induces coaggregation of carbon and silicon selfinterstitials that probably play the role of SiC nucleation centres, but do not have the thermal stability of SiC.

1. Introduction

The need for cheap starting material in terrestrial solar cell production urged development of several techniques to furnish substrate material. The edge-defined film-fed growth (EFG) method for pulling single crystals of predetermined cross-section was initially used in the growth of sapphire [1], and now is one of the prospective techniques used in low-cost production of quality silicon crystals. CO and CO_2 gasses are used as purging gasses [2] to modify structure and improve the electronic properties of ribbons for the purpose of making solar cells. Improvements obtained are due to changes in ribbon carbon and oxygen concentrations. Ambient gas composition variation have already been used to produce changes in carbon and oxygen concentration in silicon crystals grown by float zone [3] and Czochralski [4] methods.

The reaction of CO with a silicon melt can produce SiC, SiO_2 and SiO with typical growth system temperatures (1685 K) and reacting gas partial pressures ($\sim 10^{-3}$ atm) as shown previously [5]. The meniscus melt already has a high level of incorporated carbon because EFG material is grown with graphite crucibles and dies. Therefore, additional carbon supplied from the ambient atmosphere will not tend to go into solution if the melt is saturated. Thus formation of SiC may accommodate the carbon brought to the meniscus surface by the gas [6].

When studying carbon incorporation from the interface boundary layer, Kalejs and Chalmers [7] proposed a model that involves nucleation and growth of SiC nanoprecipitates on the liquid–solid interface occurring under conditions of hypereutectic solidification. They found that the precipitate radius could reach 10 μm under appropriate conditions.

Large-grain SiC ($\geq$ 10 μm) particles were found at the ribbon [8] surface. However, submicrometre precipitates were not, even with high-resolution transmission microscopy with resolution capabilities down to 5–10 nm sizes [9]. The formation of larger grains was attributed to erosion of the graphite dies [10].

Redistribution of impurities across the sheet is not symmetrical and strongly depends on process parameters [8], because asymmetrical (displaced) dies have been used recently in the growth process [11]. Strong asymmetry obtained in carbon concentration would favour SiC formation.

This paper discusses thermal stability as well as certain properties of a thin film formed on one side of EFG polycrystalline silicon ribbon, during ribbon growth.

2. Experimental procedure

The EFG polycrystalline silicon samples used in our experiments were supplied by Mobil Solar Energy Corp. All samples examined were p-type, boron doped, with 5–10 Ωcm resistivity, and were about 500 μm thick. All were grown in ribbon-like form with large monocrystalline grains (a few milimetres across) grown parallel to each other and perpendicular to the surface of the ribbon.

Room temperature infrared (IR) spectra in the wave number range from 5000–400 cm^{-1}, were taken with a Bruker Fourier transform IR (FTIR) spectrometer

* *Permanent address*: R. Boskovic Institute, P.O. Box 1016, YU-41000 Zagreb, Yugoslavia.

0022–2461/91 $03.00 + .12

113 v. A globar source with a cooled mercury cadmium telluride detector and KBr beam spliter were used. The instrumental resolution was 4 cm^{-1}.

A differential technique was employed in the transmission measurements with float zone oxygen and carbon-free monocrystalline silicon wafer as reference.

Reflectivity measurements at near normal incidence were performed using a gold mirror as reference.

Spectroscopic ellipsometer data were obtained with a MOSS rotating-polarizer spectroscopic ellipsometer. The two ellipsometer parameters $\tan\psi$ and $\cos\Delta$ were measured as a function of wavelength in the range 300–800 nm at 75° incidence angle. Standard calibration procedure was performed prior to measurement. The analyser position was tracked to the value of ψ in order to optimize the S/N ratio during measurements.

Secondary ion mass spectrometry (SIMS) measurements were carried out using a CAMECA IMS 4F ion microprobe. Cs^+ primary ions at 10 kV accelerating voltage and 4 mA cm^{-2} current density, rastered to 150 × 150 μm^2 were used to detect ^{16}O and ^{12}C in negative mode.

3. Results

Fig. 1 shows the absorbance spectrum in the range 1400–400 cm^{-1} of an as-received EFG sample grown in an argon atmosphere with CO gas added, obtained with a differential technique with respect to float zone (FZ) oxygen and a carbon-free sample. Different peaks could be clearly observed from the spectrum. The pronounced peak at 605 cm^{-1} indicates the presence of substitutional carbon in the bulk of material in the concentration of $c(C_s) = 1.2 \times 10^{18}$ atoms/cm^3. The calibration constant used was $\chi(C_s) = 1.1 \times 10^{17}$ atoms/cm^3 (ASTM Method F 121-81).

The broad peak ranging from 1000–1100 cm^{-1} with shoulder up to 1200 cm^{-1} indicates the presence of various oxygen complexes, particularly an SiO_x phase. Dipping of the as-received sample in HF did not remove this peak, thereby suggesting that it was not due to the surface oxide present. The narrow, high peak at 794 cm^{-1} was attributed to the existence of SiC phase [12]. This attribution is not surprising because the presence of SiC particles could originate

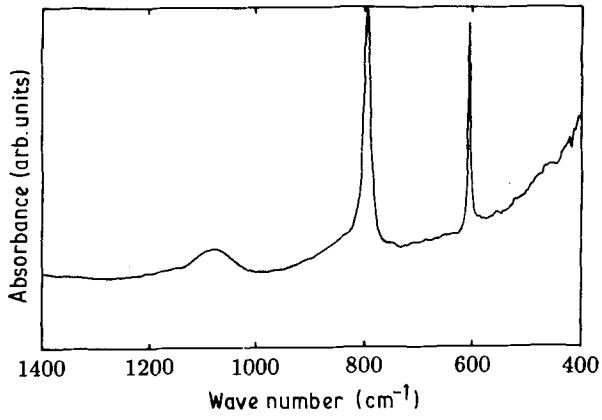

Figure 1 Differential IR transmittance spectrum of as-received EFG poly-Si sample.

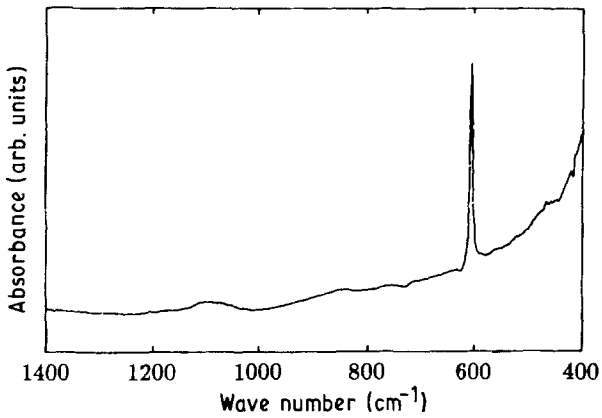

Figure 2 Differential IR transmittance spectrum of EFG poly-Si sample after removing about 5 μm of the surface layer.

from the specific conditions employed in ribbon production as described above.

Fig. 2 shows an IR absorbance spectrum of the same sample after about 5 μm of the surface layer was etched off with planar etch. There was no significant change in the 605 cm^{-1} peak intensity, indicating that this treatment did not substantially alter the concentration of substitutional carbon.

Although the carbon concentration close to the surface in this type of material (in a layer about 1 μm thick) has been found [8] to increase by a few orders of magnitude, the major contribution to this peak comes from the bulk of the unaltered material.

The broad peak from 1000–1100 cm^{-1} almost completely vanished and the high peak at 794 cm^{-1} disappeared completely. This indicates that complexes that give rise to the IR absorption spectrum in this range are in the layer close to the surface.

The reflectance in the same spectral region of the as-received sample is shown in Fig. 3. The peak at 794 cm^{-1} (curve B) is in good agreement with relevant literature data [13] for a cubic SiC layer. The negative peak close to 600 cm^{-1} in the same spectrum could be explained with a model of two-face reflection and is due to two-phonon absorption. Curve A represents reflection on the other surface. It is worth noting that this spectrum peak at 794 cm^{-1} is negative, indicating that this surface lacks SiC-like aggregates which could give rise to the aforementioned peak.

Spectroscopic ellipsometry measurements were performed on the same sample and are shown in Figs 4 and 5. Measurements reported in Fig. 4 are for side A which had no SiC-like aggregates, as shown by IR reflectance. $\tan\psi$ and $\cos\Delta$, n and k values shown in Fig. 4a and b, respectively, are similar to those of pure monocrystalline silicon. This confirms that this side consists of high quality polycrystalline silicon and is free of SiC-like aggregates. Measurements of $\tan\psi$ and $\cos\Delta$, performed on the other side are shown in Fig. 5. Comparison of these results with those of Fig. 4 confirms that side B does not only contain polycrystalline silicon. IR measurements lead us to conclude that this surface of the sample is covered with cubic SiC film. Values of $\tan\psi$ and $\cos\Delta$ of cubic SiC film 100 nm thick on monocrystalline Si substrate are plotted in Fig. 6, for verification. These values were obtained

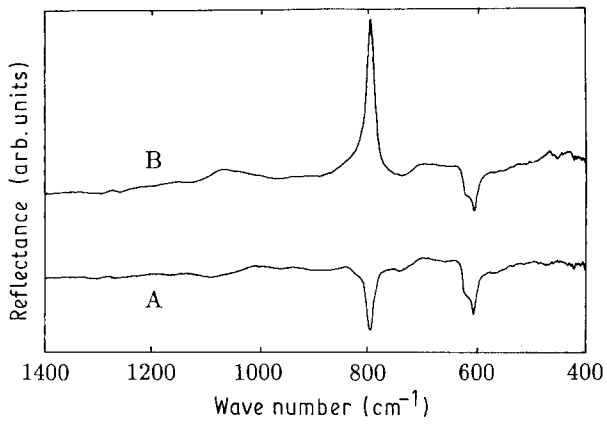

Figure 3 Differential IR reflectance spectra of (A) the pure Si side of the sample and (B) the side with SiC-like structures.

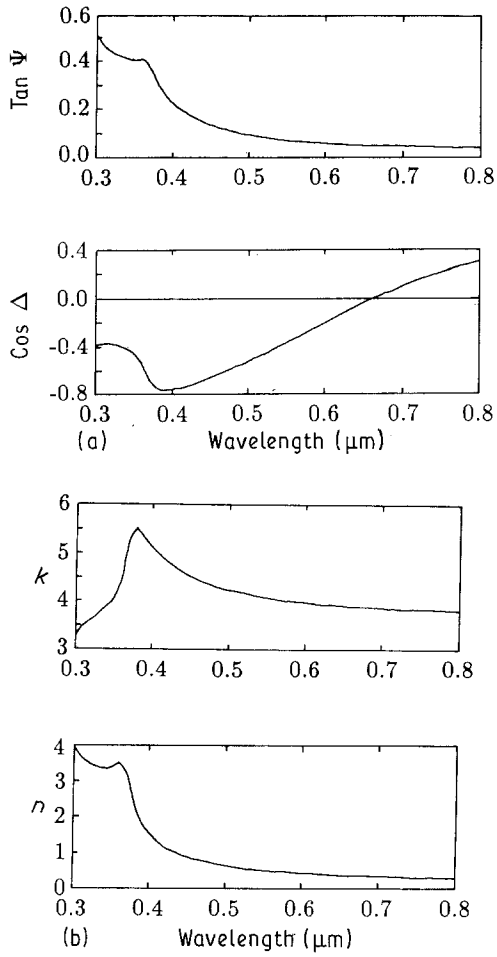

Figure 4 (a) Measured tanψ and cosΔ data for the pure Si side of the sample and (b) calculated n and k values for the same side.

numerically from data for n and k reported in the literature [14]. The values presented in Figs 5 and 6 differ greatly. This indicates that our polycrystalline Si sample does not have a pure SiC layer. Indeed, if we assume that there is a transparent layer of SiC on the surface of the silicon and calculate values for n and thickness from data for tanψ and cosΔ shown in Fig. 5, we do not get any significant values of these quantities.

Qualitative SIMS analysis of our samples is shown in Figs 7–9. Fig. 7 shows SIMS profiles for C and O taken on the as-received sample on side A (pure Si surface) and on side B (Si surface covered with film of

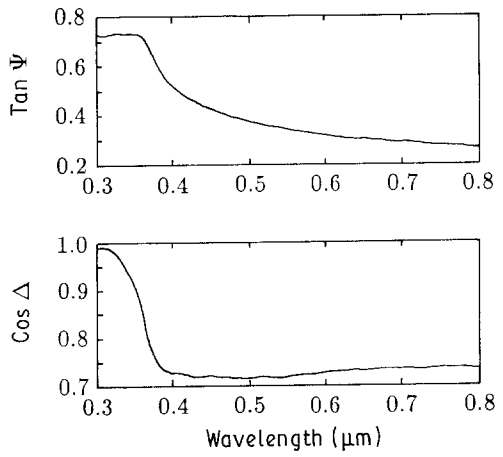

Figure 5 Measured tanψ and cosΔ values for the side with SiC-like structures.

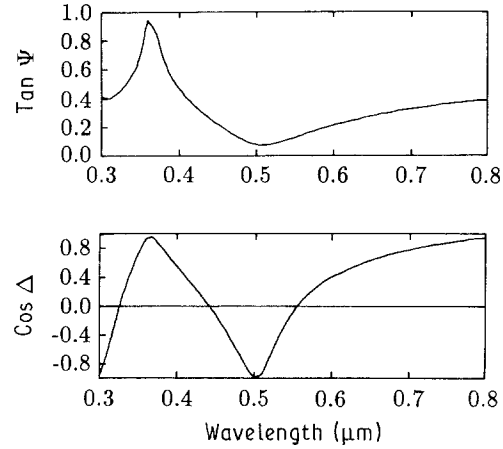

Figure 6 Calculated tanψ and cosΔ values for 100 nm thick layer of cubic SiC on crystalline Si substrate.

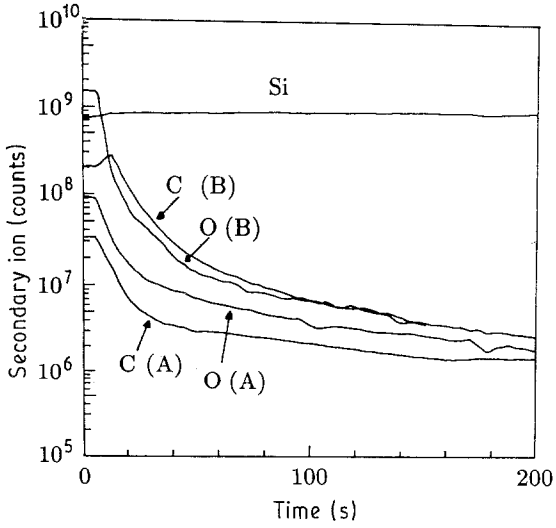

Figure 7 SIMS depth profiles for C and O of the as-received sample on side A (pure Si face) and side B (surface covered with SiC-like structures).

SiC aggregates). A significant increase in the C and O concentration can be observed close to the clean silicon surface as well. These concentrations are significantly higher and with more extended tails on side B, i.e. on the surface covered with SiC-like aggregates. It is also worth noting that the peak concentration of C

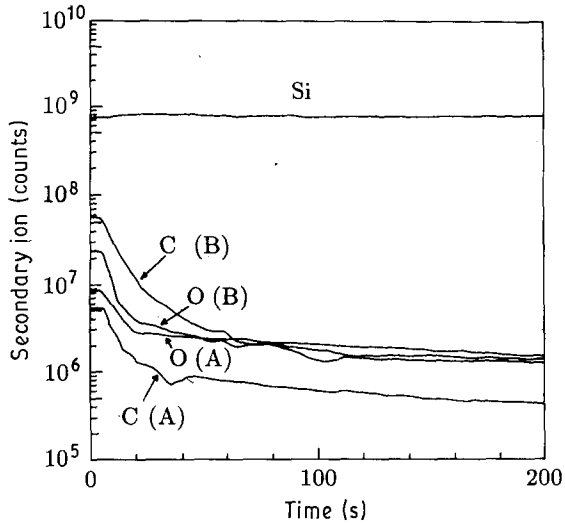

Figure 8 SIMS depth profiles for C and O of the sample on side A (pure Si face) and side B (surface covered with SiC-like structures), heated in air for 72 h.

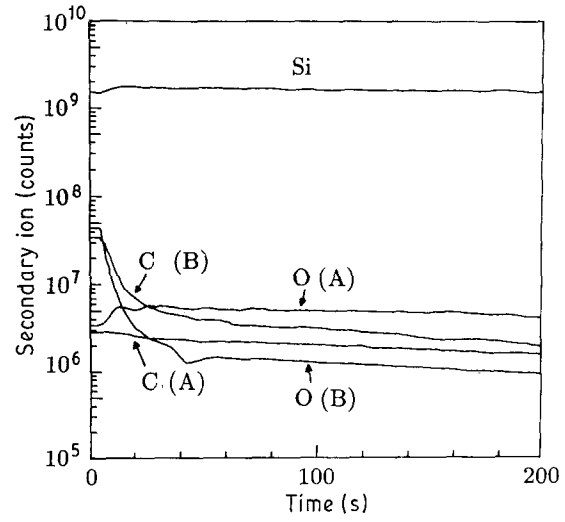

Figure 9 SIMS depth profiles for C and O for the sample after removal of approximately 5 μm of the surface layer on side A (pure Si face) and side B (surface covered with SiC like structures).

on side B does not coincide with the surface, but is approximately 0.05 μm below it. C and O profiles taken after the sample has been heated for 72 h at 650 °C in air are shown in Fig. 8. It should be mentioned that samples were etched in HF solution in order to remove the oxide layer formed on the surface after this heat treatment in air. As shown in Fig. 8, both C and O concentrations in the layer close to the surface diminished due to their outdiffusion. Furthermore, the decrease in concentration is unexpectedly more pronounced on side B of the sample, particularly for oxygen.

Fig. 9 shows SIMS profiles of the as-received sample from which approximately 5 μm of the surface layer was removed. As shown in the figure, the carbon concentration is constant on side A. On side B the large carbon pile up close to the surface as found in non-treated material is significantly reduced in depth and concentration.

The effect of thermal treatment on SiC-like aggregates is shown in Fig. 10. The figure shows the decrease

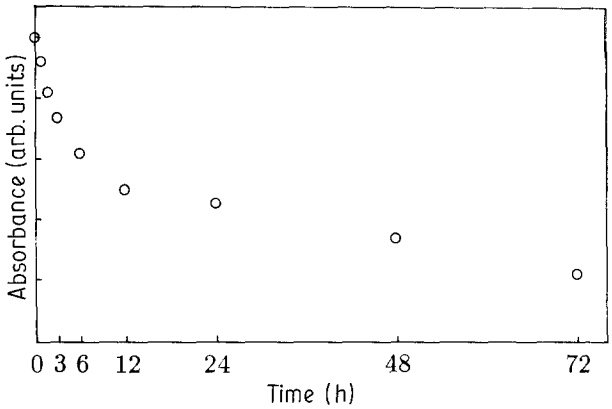

Figure 10 Relative change in 794 cm^{-1} peak height upon annealing at 650 °C in air.

of 794 cm^{-1} absorbance peak height, due to isothermal annealing at 650 °C in air. This indicates that the corresponding structure giving rise to the aforementioned IR peak is not stable upon heating at 650 °C and either dissolves or decomposes.

4. Discussion

A broad peak in the range 1000–1100 cm^{-1} as mentioned before, is attributed to SiO_x-like agglomerates. From Figs 1 and 2 it is clear that they are found in the layer close to the surface. This peak is also not due to the oxide layer grown on the surface because it cannot be removed when dipping sample into HF solution. Furthermore, Pivac and Desnica [15, 16] found that this peak is rapidly dissolved upon thermal treatment at 650 °C in a flowing dry nitrogen atmosphere. Therefore this indicates that it is not due to the stable SiO_x phase, but due to SiO_x-like aggregates that may serve as a nucleation centre for further SiO_x phase growth. It is known [8] that EFG material has a very high concentration of structural defects such as grain boundaries and subgrain boundaries, and exhibits a subsurface defect structure. It is very likely that those defect structures served as a site for oxygen agglomeration in SiO_x-like structures that dissolve upon low-temperature thermal treatment.

Furthermore, in Fig. 1 a pronounced peak at 794 cm^{-1} is shown, attributed [12] to SiC, as mentioned before. This is in accordance with the literature data: Spitzer *et al.* [13, 17] and Holm *et al.* [18], found that crystalline SiC film 0.06 μm thick grown on an Si substrate has a strong absorption band at 794 cm^{-1}, as well as a strong reflection peak at the same position. This is exactly the same as seen in Figs 1 and 3. From Figs 1–3 we can conclude that the observed peak is not due to SiC phase present in the bulk of material, but due to the contribution of a thin film grown on only one side of the EFG ribbon.

Ellipsometric data confirm the fact that one side of the sample is pure Si substrate, because we can obtain n and k from values of $\tan\psi$ and $\cos\Delta$ that are equal to those of pure silicon. However, it does not confirm that we have an SiC layer on the other side. Fig. 5 shows that behaviour of $\tan\psi$ and $\cos\Delta$ values for the unknown layer on our sample is substantially different

from the respective data calculated from the literature [14] values of n and k of 100 nm SiC film on monocrystalline silicon substrate. Therefore, we were led to conclude that the unknown layer was not SiC.

In addition, we performed a Raman spectroscopic analysis on surface B of the sample. We only obtained the characteristic spectrum of pure monocrystalline silicon without the characteristic peaks that could be attributed to any of SiC polymorphs known in the literature [19].

SIMS measurements were performed in order to understand phenomena occurring close to the surface in our material. It is clear from Fig. 7 that carbon concentration increases close to the surface on both sides of ribbon, as already reported [8]. We also noticed that carbon concentration is significantly higher on one side (the side with an SiC-like layer). However, the carbon level several micrometres beneath the surface from both sides is similar, indicating that there is no significant macroscopical variation in carbon concentration across the ribbon, as found earlier [8]. Furthermore, carbon pile up to both surfaces is not equal. The surface peak of carbon concentration for pure Si corresponds to the position of the surface, while it is about 0.05 μm below the surfaces on the other side. On the other hand, the oxygen concentration, which also increases significantly close to the surface, is much higher at the surface covered with the SiC-like layer, and its peak value corresponds to the surface.

It is very interesting to see the difference after heat treatment at 650 °C for 72 h in air. Oxygen and carbon concentrations are lower than in as-received material, but the oxygen concentration decreased in particular. Furthermore, the decrease on the side covered with the SiC-like layer seems to be greater. On the other hand, the carbon concentration decreased, preserving the ratio of the respective sides of the as-received sample. Only a small carbon pinning close to the surface remained at the pure silicon surface. A significant carbon concentration close to the surface still remained on the surface previously covered with the SiC-like layer. However, the maximum carbon concentration now corresponds to the surface, with no peak in the subsurface region.

Fig. 9 shows that carbon concentration profile was flat on both sides when the surface layer of the as-received sample was removed by chemical etching. If the layer formed on one surface is stable SiC, as concluded from IR measurements, this phase should be stable upon thermal treatment to very high temperatures. Spitzer *et al.* [13] found that no harm could be done to the SiC film at temperatures of 600–650 °C, even in an oxidizing atmosphere, i.e. they obtained a C film on an SiC layer during SiC layer preparation and they found that the C film can be removed by oxidation at temperatures in the region of 600–650 °C without oxidizing the SiC layer.

We performed a similar experiment. Fig. 10 shows the effect of isothermal heat treatment of our sample in air. We obtained results similar to those of isothermal heat treatment of the same sample at 650 °C in flowing dry nitrogen atmosphere. Therefore, although it is not very likely that the SiC layer could be oxidized in air at only 650 °C upon heat treatment, it is evident from our experiment in a nitrogen atmosphere that there is a "dissolution" of the SiC-like layer on our polycrystalline silicon sample.

We propose the following model [20] as an explanation for our experiment. Oxygen formed upon interaction of CO gas with Si melt [6] diffuses into the subsurface layer during crystal growth. It segregates there and facilitates further coprecipitation of carbon and silicon selfinterstitials, as found by Feng *et al.* [21]. This material already has carbon in supersaturation, therefore additional generation of silicon selfinterstitials causes agglomeration with carbon and acts as a SiC nucleation centre. Such nucleation centres in significant concentrations give rise to an SiC-like absorbance spectrum. However, although these centres seem to be precursors for SiC formation, they did not grow to a certain critical radius necessary for the stability of SiC precipitates. This can explain the fact that they were easily dissolved at only 650 °C upon thermal treatment in air or inert atmosphere.

5. Conclusions

We conclude that the layer formed at one surface of EFG polycrystalline silicon ribbon does not contain SiC as a well-defined and stable phase, having all structural properties of cubic SiC despite the well-defined peak in the IR absorbance and reflectance spectrum at 794 cm^{-1}. Furthermore, we proposed a model in which indiffused oxygen induced carbon and silicon selfinterstitial agglomeration in surface layer. Such agglomerates could serve as nucleation centres for SiC formation and in significant concentrations could give rise to a spectrum similar to cubic SiC. However, they do not have the stability of cubic SiC phase and can be dissolved with low-temperature thermal treatment.

Acknowledgements

This work was partially supported by Gruppo Nazionale Struttura della Materia del Consiglio Nazionale delle Ricerche. One of the authors (BP) is grateful for the support of the ICTP Programme for Training and Research in Italian Laboratories, Trieste, Italy. The authors thank Dr M. Berz, PSI, Zurich, for Raman spectroscopy measurements, and Dr J. P. Piel, SOPRA, Paris, for ellipsometric measurements and discussion.

References

1. H. E. LA BELLE Jr and A. I. MLAVSKY, *Mater. Res. Bull.* **6** (1971) 571.
2. J. P. KALEJS, M. C. CRETELLA, F. V. WALD and B. CHALMERS, in "Electronic and Optical Properties of Polycrystalline or Impure Semiconductors and Novel Silicon Growth Methods", edited by K. V. Ravi and B. O'Mara (The Electrochemical Society Proceedings, Pennington, NJ, 1980) p. 242.
3. W. KAISER and P. H. KECK, *J. Appl. Phys.* **28** (1957) 882.

4. J. A. BAKER, in "Semiconductor Silicon 1969", edited by R. R. Haberecht and E. L. Kern, (The Electrochemical Society Proceedings, Pennington, NJ, 1969) p. 566.
5. F. SCHMID, C. P. KHATTAK, T. G. DIGGS Jr and L. KAUFMAN, *J. Electrochem. Soc.* **126** (1979) 933.
6. J. P. KALEJS and L. Y. CHIN, *ibid.* **129** (1982) 1356.
7. J. P. KALEJS and B. CHALMERS, *J. Crystal Growth* **79** (1986) 487.
8. J. P. KALEJS, in "Silicon Processing for Photovoltaics II", edited by C. P. Khattak and K. V. Ravi (North-Holland, Amsterdam, 1987) p. 185.
9. D. B. AST, B. CUNNINGHAM and H. P. STRUNK, in "Grain Boundaries in Semiconductors", edited by H. J. Leamy, G. E. Pike and C. H. Seager (North-Holland, New York, 1981) p. 167.
10. J. KATCKI, *J. Crystal Growth* **82** (1987) 197.
11. J. P. KALEJS, L-Y CHIN and F. M. CARLSON, *ibid.* **61** (1983) 473.
12. J. A. A. ENGELBRECHT, *Infrared Phys.* **26** (1986) 243.
13. W. G. SPITZER, D. A. KLEINMAN and C. J. FROSCH, *Phys. Rev.* **113** (1959) 133.
14. S. A. ALTEROVITZ and J. A. WOOLLAM, in "Handbook of Optical Constants of Solids II", edited by E. D. Palik (Academic Press) to be published.
15. B. PIVAC and U. V. DESNICA, *J. Appl. Phys.* **64** (1988) 2208.
16. *Idem., ibid.* **65** (1989) 4759.
17. W. G. SPITZER, D. A. KLEINMAN and C. J. FROSCH, *Phys. Rev.* **113** (1959) 127.
18. R. T. HOLM, P. H. KLEIN and P. E. R. NORDQUIST Jr, *J. Appl. Phys.* **60** (1986) 1479.
19. H. OKUMURA, E. SAKUMA, J. H. LEE, H. MUKAIDA, S. MISAWA, K. ENDO and S. YOSHIDA, *ibid.* **61** (1987) 1134.
20. B. PIVAC, A. BORGHESI, M. MOSCARDINI, P. BOTTAZZI and U. V. DESNICA, *J. Mater. Sci. Lett.* **9** (1990) 397.
21. S. Q. FENG, J. P. KALEJS and D. G. AST, in "Oxygen, Carbon, Hydrogen and Nitrogen in Crystalline Silicon", edited by J. C. Mikkelsen Jr, S. J. Pearton, J. W. Corbett and S. J. Pennycook (Materials Research Society, Pittsburgh, 1986) p. 439.

Received 21 March
and accepted 2 August 1990